Thermodynamic investigations of the NaI-CsI, KI-CsI, and NaF-CsI pseudo-binary systems

Scuro, N. L.; Fitzpatrick, B. W.N.; Geiger, E.; Poschmann, M.; Dumaire, T.; Beneš, O.; Piro, M. H.A.

DOI
10.1016/j.jct.2024.107272

Publication date
2024

Document Version
Final published version

Published in
Journal of Chemical Thermodynamics

J. Chem. Thermodynamics 193 (2024) 107272

Contents lists available at ScienceDirect

The Journal of Chemical Thermodynamics

journal homepage: www.journals.elsevier.com/the-journal-of-chemical-thermodynamics

Thermodynamic investigations of the NaI-CsI, KI-CsI, and NaF-CsI pseudo-binary systems

N.L. Scuro [a,*], B.W.N. Fitzpatrick [a], E. Geiger [a,b], M. Poschmann [a,b], T. Dumaire [c,d], O Beneš [c], M.H.A. Piro [a]

[a] Department of Energy and Nuclear Engineering, Ontario Tech University, Oshawa, ON, Canada
[b] Canadian Nuclear Laboratories, Chalk River, ON, Canada
[c] European Commission, Joint Research Centre, Institute for Transuranium Elements, Karlsruhe, BW, Germany
[d] Radiation Science and Technology Department, Delft University of Technology, Delft, ZH, The Netherlands

A B S T R A C T

The present study describes the thermodynamic assessment of three pseudo-binary systems relevant to CsI solubility in molten iodide salts: KI-CsI, NaI-CsI, and NaF-CsI. The motivation for this study was to corroborate a single previously reported data set of the NaI-CsI system, resolve inconsistencies reported by two different data-sets of the KI-CsI system, and generate new experimental data on the NaF-CsI system. Equilibrium data for all systems were obtained using Differential Scanning Calorimetry. Thermodynamic treatments of the three pseudo-binary systems were revised using the CALPHAD method with the thermodynamic software FactSage and Thermochimica. Both experimental and computational investigations provide increased confidence in the thermochemical behaviour of CsI in Molten Salt Reactor nuclear systems.

1. Introduction

Molten salt thermodynamics plays an important role in numerous metallurgical and nuclear applications, particularly in the conceptual design of Molten Salt nuclear Reactors (MSR). Understanding the thermodynamics of multi-component mixtures of molten salts is especially crucial in the context of reactor safety: the fuel and coolant are often the same in many MSR designs [1], and therefore there is no physical barrier. This emphasizes the need for accurately quantifying the source term (*e.g.*, both of activated corrosion and fission products).

While significant progress has been made in investigating the thermochemistry of fuel and fission products in fluoride salts [2–6] knowledge gaps remain largely, due to the numerous chemical species and fission products present during operation of MSR. Furthermore, many experimental investigations of these salts have not been independently corroborated and, in some cases, multiple reports are in disagreement with one another. These factors pose challenges to the quality assurance of molten salt thermodynamic analyses. Systems involving CsI are of particular interest for better understanding iodine and cesium chemistry in an MSR, as they are volatile fission products and therefore important in the context of reactor safety (*e.g.* source term) [5,7,8]. The radiological impact of iodine makes this element one of the most important fission products to take care of in nuclear waste management. As a result of its high chemical reactivity, iodine is present in different forms in the radioactive effluents. For example, in Light-Water Reactors (LWR), iodine is stable as molecular iodine (I_2 gas) but it can also be associated with organic and aerosol compounds [9,10]. As iodine may also react with fission products such as cesium, the interaction of cesium iodide with relevant chemical species (such as NaI and KI) and its solubility in molten salt coolant species (such as NaF) needs further investigation. Given the lack of experimental data and thermodynamic models for CsI with the latter species, as well as the need for investigation using modern Differential Scanning Calorimetry (DSC) techniques for the development of the Joint Research Centre - Molten Salt Database (JRCMSD) [11], this work focused on investigating three pseudo-binary systems: NaI-CsI, KI-CsI, and NaF-CsI.

Measurements pertaining to the NaI-CsI system have been previously reported by Samuseva and Plyushchev [12], and by Il'yasov and Berman [13] using Differential Thermal Analysis (DTA) and visual-polythermal methods. According to Sangster and Pelton [14], the melting point of CsI reported by Samuseva and Plyushchev [12] is 8 °C higher than the generally accepted value (640 °C against 632 °C, respectively) and the reported liquidus points show significant dispersion near the eutectic. At the same time, the comparison of liquidus curves between Samuseva and Plyushchev [12] and Il'yasov and Berman [13] presents poor agreement, and the experimental uncertainty varying from 1 °C to 80 °C. Due

* Corresponding author.
E-mail address: nikolas.scuro@ontariotechu.net (N.L. Scuro).

https://doi.org/10.1016/j.jct.2024.107272
Received 17 August 2023; Received in revised form 29 January 2024; Accepted 6 February 2024
Available online 13 February 2024

Table 1
Literature review of KI-CsI data.

Eutectic [°C]	KI [mol%]	Solid Phases	Analysis	Ref
516 (± 40 °C)	45.0	unclear	Exp	[15]
494	21.0	unclear	Exp	[16]
559	30.0	unclear	Exp	[18]
555 (± 1 °C)	38.6	no evidence	Exp	[17]
536	39.0	CsI and KI	Model	[14]

to the better agreement among their reported results, Sangster and Pelton [14] recommended the results of Il'yasov and Berman [13] as the basis for their thermodynamic modelling. It is important to state that the study of Samuseva and Plyushchev [12] did not observe any solid solubility between CsI and NaI phases. The thermodynamic model from Sangster and Pelton [14] for this system predicts a eutectic point at 428 °C and 48.5 mol% of CsI [14]. The calculated liquidus follows the general trend of the experimental results of Il'yasov and Berman [13], but does not fully coincide with the experimental values, resulting in a maximum error of the calculated phase diagram of ± 20 °C, which gives motivation for further investigation.

Phase boundary data in the KI-CsI system have been reported by Samuseva and Plyushchev [15] and Il'yasov et al. [16] using DTA, and Sato et al. [17] who used Thermo-Gravimetric Analysis (TGA) and DTA, which markedly contrast one another regarding the eutectic temperature and solid solubility between CsI and KI. A literature review of this system is summarized in Table 1, where inconsistencies for the eutectic point and the presence or not of solid phases are indicated. Different methodologies and techniques also show significant differences for the average temperature value. According to Sangster and Pelton [14], early results obtained by Samuseva and Plyushchev [15] show large discrepancies in eutectic point (516 (± 40 °C)) to Il'yasov et al. [18] (559 °C). Years later, Sato et al. [17] reported a eutectic temperature of 555 °C [17] with consistent results of miscibility of KI and CsI, which were not observed in previous studies [15,16,18]. It is important to state that the liquidus curvatures of all data sets are quite different from one another. The only available thermodynamic model of KI-CsI was proposed by Sangster and Pelton [14] who considered the general trend of results observed by Samuseva and Plyushchev [15]. The latter includes experimental data on the solid miscibility of KI and CsI.

To the best of the authors' knowledge, there are no existing experimental measurements reported in the open literature about the NaF-CsI pseudo-binary system. This lack of data is not surprising, as these systems do not share common anion or cation pairs (i.e., it is a reciprocal salt). Due to the possible use of fluoride salt species in the molten salt coolant system, and the formation of fission products (CsI), the solubility between different anion or cation pairs is probable and their interaction should be investigated.

The objective of this study was to fill knowledge gaps on the NaI-CsI, KI-CsI, and NaF-CsI systems by conducting DSC measurements, corroborating previously reported measurements, and addressing any discrepancies of previously reported experimental data. The majority of DSC measurements were performed at Ontario Tech University (OTU) with a few additional measurements performed at the Joint Research Centre (JRC, Karlsruhe) to corroborate some findings. Additionally, thermodynamic models were developed for these systems to integrate them into a larger thermodynamic database (*i.e.* JRCMSD). The methodology employed in the experimental work is described in §2, the development of each thermodynamic model is detailed in §3, the results and discussion of both the experimental and model data are presented in §4, and conclusions are drawn in §5.

2. Experimental Methodology

Experiments performed at OTU utilized the methodology, equipment, and procedures described in detail by Lipkina et al. [19]. In the subsections, only the notable differences, significant aspects to emphasize, and unique hypotheses adopted in this study will be described. At the end of this section, the methodology adopted by JRC is presented.

Table 2 describes all sample details, such as chemical name, source, purity, purification method, equipment, and sample holders. Given the hygroscopic nature of most fluorides, and similarly for iodine salts, an additional dehydration/purification process was applied to each end-member. Samples were prepared, ground, and dehydrated at specific temperatures inside an MBRAUN glovebox-controlled environment using argon, with O_2 and H_2O levels at a maximum of 5 ppm, typically below 0.5 ppm. OTU samples were dehydrated at 200°C for 2 h, and at JRC, at 300°C for 4 h. Later, to evaluate the purity, samples were run in sealed crucibles, and DSC signals were analyzed. All components

Table 2
Chemical compound's names, formula, vendor's source, and purification aspect.

Chemical Name	Formula	Source	Initial Mole Fraction Purity*	Purification Method	Final Mole Fraction Purity
Sodium iodide	NaI [20]	Sigma–Aldrich	99.999%	Dehydration	DSC[a]
Cesium iodide	CsI [21]	Sigma–Aldrich	99.999%	Dehydration	DSC[a]
Potassium iodine	KI [22]	Sigma–Aldrich	99.999%	Dehydration	DSC[a]
Sodium fluoride	NaF [23]	Sigma–Aldrich	99.99%	Dehydration	DSC[a]
Cesium iodine	CsI [21]	Thermo Fisher Scientific Inc.	99.999%	Dehydration	DSC[b]
Potassium iodine	KI [22]	Thermo Fisher Scientific Inc.	99.99%	Dehydration	DSC[b]
Sodium fluoride	NaF [23]	Carl Roth Gmbh & Co. kg	99.995%	Dehydration	DSC[b]

[a] Samples used at Ontario Tech University were tested using the DSC-TGA mode of a Netzsch Jupiter 449 F1 Simultaneous Thermal Analyzer (STA), SiC furnace with a Type S TGA-DSC sample carrier with a Pt/Rh head (product No. HTP40000A54.010–00).
[b] Samples used at the Joint Research Centre were tested using a SETARAM Multi-Detector High-Temperature Calorimeter with an S-type DSC detector.
* **All initial mole fraction purity are based on metal trace basis.**

Table 3
Comparison between reference melting point, with calculated pressurized environment of sealed crucibles for pure end member components.

Compound	Ref. Melting Point	Exp. Melting Point	Calculated Pressure
CsI	632.0 °C	627.1 ± 10 °C (5 °C/min)	3.06 atm
NaI	661.0 °C	657.9 ± 10 °C (5 °C/min)	3.16 atm
KI	681.0 °C	679.0 ± 10 °C (2 °C/min)	3.24 atm
		680.2 ± 10 °C (5 °C/min)	3.24 atm
NaF	993.0 °C	997.4 ± 10 °C (5 °C/min)	4.33 atm

* CsI, NaI, KI and NaF presented temperature uncertainty, $u(T) = \pm 10$ °C for liquidus at 5 and 2 °C/min, for a standard uncertainty with 0.68 level of confidence.

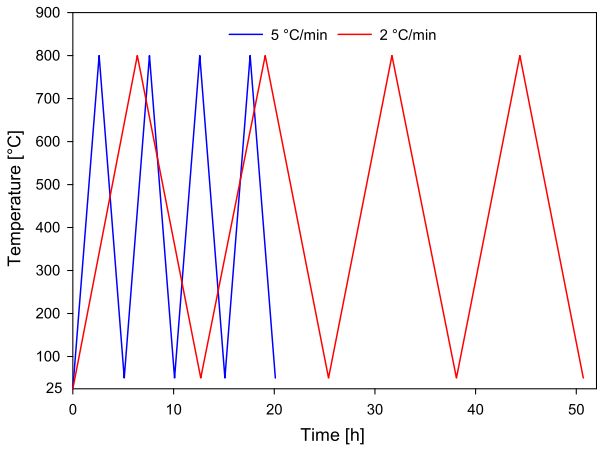

Fig. 1. 2 °C/min and 5 °C/min temperature sequence program for KI-CsI samples.

presented clear peaks, without oscillations, indicating the absence of impurities, and the melting temperatures matched those provided by the vendors and referenced in the literature. (see Table 3).

Although Table 2 represents pure end members, information on mixture components for CsI-NaI, KI-CsI, and NaF-CsI systems can be found in Tables 9–11, respectively, indicating which measurements have been done for each institution.

2.1. Crucible Design

As commercially available DSC crucibles do not meet the requirements for the measurements conducted in this study mainly due to the chemical reaction of salts with crucible walls, a modified version of the Netzsch SS316L crucible, originally developed by Piro et al. [24], was utilized for all measurements at OTU. This design incorporates the use of Netzsch crucible and lid, along with a custom Ni-201 gasket and liner that demonstrated no interaction between the crucible and salt specimens. Crucibles and lid were sealed using a Netsch sealing press (product No. 6.239–2-92.4.00) with an adjustable torque wrench.

For measurements done by JRC, an in-house design has been used, which is described in detail in the study of Beneš et al. [25]. The crucible is made of stainless steel, but an inner liner of nickel is used, avoiding chemical interaction with the salt sample.

2.2. DSC Temperature Calibration

The calibration procedure was carried out using the Netzsch Temperature Calibration software [26–29], following the method and recommendations outlined by Piro et al. [24]. For calibration, a combination of commercially available Netzsch calibration sets of pure metals (In, Sn, Pb, Ag) (part No. 6.223.5–91.3.00) and two calibration sets of inorganic compounds (CsCl and K_2SO_4) were specifically selected due to their lack of chemical interaction with Ni-201 and their suitability for calibrating the temperature range used in this study (250 °C to 1100 °C). Two different heating rates were employed: 5 °C/min and 2 °C/min to investigate if lower heating rates would give clearer and easier-to-interpret signals when compared to 5 °C/min DSC signals. The uncertainties on the instrument calibration are discussed in Section 2.5.

It is worth noting that, despite the DSC measurements occurring under atmospheric pressure, the internal pressure of the sealed crucible increases with the temperature rise. A simplified calculation, adhering to the ideal gas law and considering the volume of argon gas inside the crucible, was performed. It was estimated that the pressure could reach up for the following values, taking as an example, the melting point of the pure components:

The maximum temperature tested was 1250°C, corresponding to 5.18 atm. Given that no notable variations were observed for the pure components, it is extrapolated that the entire temperature range studied did not exhibit significant changes with the increased pressure.

Table 4
Error analysis of all thermodynamic systems and sources of error, for standard uncertainty, with 68% confidence interval

Error Source	CsI-NaI [°C]	KI-CsI [°C]	NaF-CsI [°C]
Netzsch DSC Thermocouple	± 0.4	± 0.4	± 0.4
DSC Temperature Reading (5 °C/min)	± 0.4	± 0.5	± 0.1
DSC Temperature Reading (2 °C/min)	± 0.4	± 0.5	± 0.1
Calibration Curve (5 °C/min)	± 1.6	± 1.6	± 1.6
Calibration Curve (2 °C/min)	± 2.9	± 2.9	± 2.9
Standard Deviation for Polymorphic	-	± 0.7	-
Standard Deviation for Eutectic		± 1.8	
Standard Deviation for Liquidus		± 4.9	
Extrapolated Eutectic to 0 °C/min		± 4.6	
Extrapolated Liquidus to 0 °C/min		± 8.1	

2.3. DSC Measurements at Ontario Tech University

The DSC temperature program was set to identify possible phase transitions, considering the melting and no-boiling temperatures for each end-member (NaI, CsI, KI, NaF). For the NaI-CsI system, temperatures ranged between 300 °C to 800 °C. For the KI-CsI system, where possible solid phase solutions were expected, the temperature ranged between 50 °C to 800 °C, as illustrated by Fig. 1. For the NaF-CsI system, the temperature ranged between 400 °C to 1200 °C.

Similar to the temperature calibration analysis, NaI-CsI, KI-CsI, and NaF-CsI tests were set to four heating cycles to better analyze DSC signals (Fig. 1). Results from the first cycle were discarded due to the salt mixture not being yet in thermodynamic equilibrium. Thus, all onset and offset temperatures presented for each sample were determined by averaging the remaining heating cycles. Samples whose composition was close to the eutectic point were run at a lower heating rate of 2 °C/min (instead of 5 °C/min) for investigation of possible improved precision. For the KI-CsI system, several mixtures were analyzed at both heating rates to study the sensitivity of the on-set and off-set temperatures along each heating cycle.

Sample compositions were varied to investigate their impact on DSC signals. In a previous study, a sample composition of 50 mg was considered optimal for obtaining clear phase transition and melting temperature analysis [19,30]. However, for some samples in the KI-CsI system, a sample composition of up to 100 mg was used to investigate if an improved signal sensitivity could eliminate possible overlapped signals in specific regions. This investigation is detailed in the subsequent sections for each system.

2.4. DSC measurements at JRC

Additional samples were prepared at JRC using commercially available KI, NaF, and CsI end-members, to create three selected pseudo-binary mixtures of KI-CsI (20–80 mol%, 31–69 mol%, and 80–20 mol%) and NaF-CsI (90–10 mol%, 70–30 mol%, and 50–50 mol%) compositions.

The calibration method adopted by JRC is similar to that of OTU. Additional samples done by JRC followed a very similar procedure for all described steps but with heating rates of 5 °C/min and 10 °C/min, as heating rates of 1 and 2.5 °C/min resulted in increased background noise without showing additional DSC signal features. The reported eutectic and liquidus temperatures are the average of 3 to 6 measurements on each sample. Tests for the KI-CsI system have been performed in the range of 20 °C to 850 °C and NaF-CsI between 20°C to 1250 °C. The uncertainty of measurements done at JRC is ± 5 °C for the eutectic equilibria and ± 10 °C for liquidus temperatures. The increased uncertainty of the latter is mainly due to the use of the DSC heat flow signal for

Table 5
Temperature differences between phase transitions ($T_{2\ K/min}$ - $T_{5\ K/min}$), between heating rates, in the KI-CsI system.

X_{KI}	Possible Polymorphic [°C]	Eutectic [°C]	Liquidus [°C]
0.039	-	−2.0	−7.0
0.070		0.0	−5.4
0.110	−0.7		−4.9
0.150		0.0	0.7
0.195	−2.2	−7.6	−6.9
0.270	0.8		−4.8
0.309		−0.7	−5.0
0.703		−0.7	−5.1
0.951		−1.3	−5.4
Average	± 0.7	± 1.8	± 4.9

* Internal pressures within the hermetically sealed SS crucibles were not monitored but showed no influence on pure component's melting temperature for up to 3.24 atm at 680 °C. KI-CsI mixture samples presented temperature uncertainty, $u(T) = \pm 5$ °C and ± 6 °C for eutectic, and ± 10 °C and ± 10 °C for liquidus, for at 5 and 2 °C/min, respectively. Mixture uncertainty was evaluated to be $u(x_{i-j}) = \pm 0.13$ mol% for the same standard uncertainty. Uncertainty is considered a 0.68 level of confidence.

determinining equilibria temperatures, which is typically much broader than the sharp onset of the eutectic (or melting) DSC features.

2.5. Experimental error analysis OTU

The uncertainty associated with the sample composition is determined to be approximately ±0.13 mol%. This uncertainty arises from two main sources. Firstly, it stems from the cleaning process of the crucible edges just before sealing it. During this step, very small amounts of salts are removed, which can have an impact on the overall composition measurement. Secondly, there is a possibility that minor amounts of salts may accidentally drop onto the anti-static boat while pouring salts into the crucible, resulting in a slight variation between the composition being measured at that moment and the composition after cleaning the anti-static boat. These factors can contribute to the general uncertainty associated with the measured sample composition.

The temperature error associated with this study, presented in Table 4, has been calculated as a combination of the cross-error (Eq. 1 between (i) the standard instrumental uncertainty in temperature measurement of the Netzsch DSC thermocouples, (ii) the standard deviation between all DSC signals associated with all the temperature readings for each phase transition (which varies between each thermodynamic system and the number of heating cycles, ranging from two to three), (iii) the error associated with the calibration curve for both heating rates and (iv) the standard deviation between differences for the eutectic and liquidus readings between 2 °C/min to 5 °C/min. Regarding the latter, only the results for the KI-CsI system are presented in Table 4 as the elevated number of measurements made such analysis possible.

$$u(T) = \sqrt{\sum_{i=1}^{n} c_i u(x_i)^2} \quad (1)$$

where $u(T)$ [°C] is the combined uncertainty for the temperature values of each thermodynamic system, combining each known uncertainty $u(x_i)$ [°C] in quadrature, and c_i represents the sensitivity coefficient and is equal to 1 since the uncertainty contributors are used in the same units of measurement [°C].

Details about the possible polymorphic, eutectic and liquidus error obtained from KI-CsI system are presented in Section 2.5.1. Then, at the end of the same section, the final resultant error for each system and heating rate is presented.

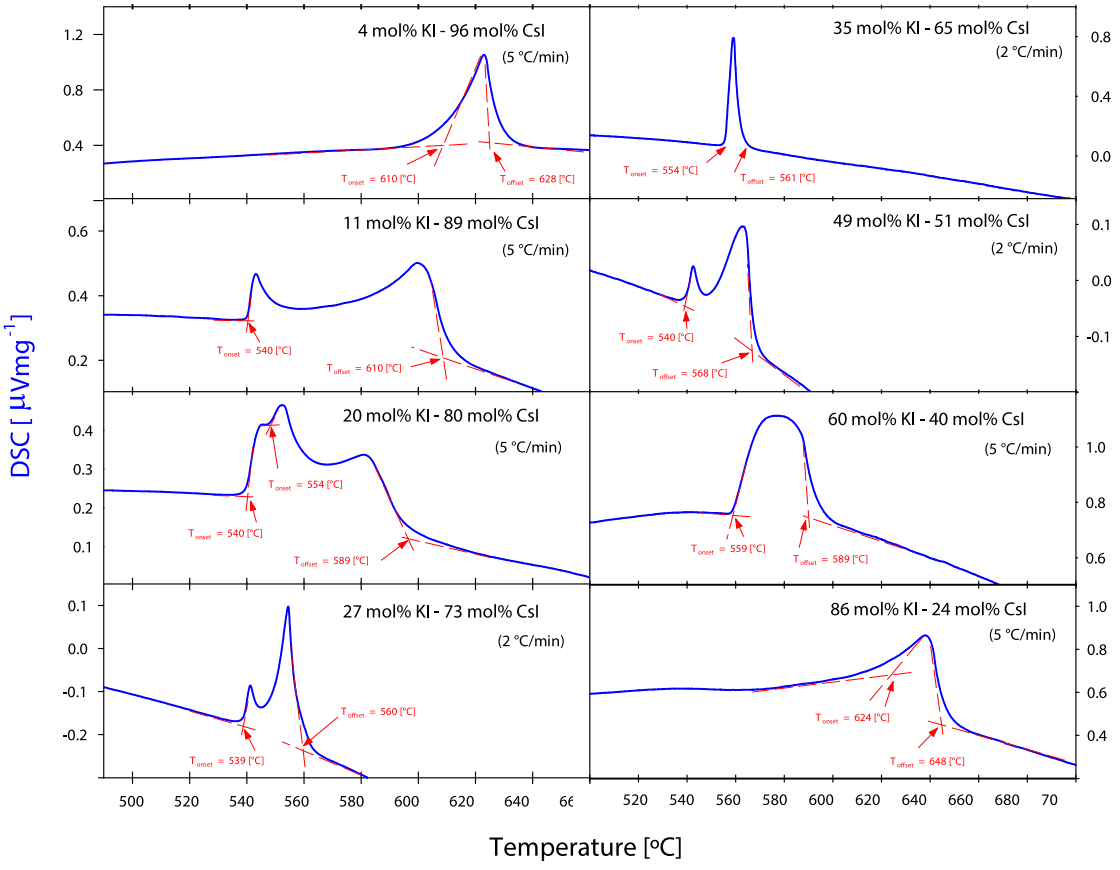

Fig. 3. Simplified KI-CsI DSC Signals.

Table 6
KI-CsI eutectic and liquidus data extrapolation to 0 °C/min. Standard uncertainty was adopted, with 68% confidence interval.

X_{KI}	0 °C/min	2 °C/min	5 °C/min	Eutectic ΔT_{Max} [°C]	Liquidus ΔT_{Max} [°C]
0.039	616.8	621.4	628.4		−11.6
0.070	612.9	616.6	622.0		−9.1
0.110	602.8	606.0	610.9		−8.1
0.150	553.6	553.6	553.6	0.0	
0.150	608.6	608.1	607.4		1.2
0.195	548.5	553.6	561.2	−12.7	
0.195	584.7	589.3	596.2		−11.5
0.270	556.6	559.8	564.6	−7.9	
0.309	553.4	553.9	554.6	−1.2	
0.309	558.7	562.3	567.3		−8.6
0.703	558.2	558.7	559.5	−1.3	
0.703	610.0	613.5	618.6		−8.6
0.951	667.9	671.2	676.6		−8.7
Average				−4.6	−8.1

*Internal pressures within the hermetically sealed SS crucibles were not monitored but showed no influence on pure component's melting temperature for up to 3.24 atm at 680 °C. KI-CsI mixture samples presented temperature uncertainty, $u(T) = \pm 5$ °C and ± 6 °C for eutectic, and ± 10 °C and ± 10 °C for liquidus, for at 5 and 2 °C/min, respectively, for 0.68 level of confidence. Mixture uncertainty was evaluated to be $u(x_{i-j}) = \pm 0.13$ mol% for the same standard uncertainty.

2.5.1. Sample composition and heating rate influence on DSC signals

Detailed error analysis for the heating rates was conducted for the KI-CsI system, and the results are presented in Table 5. For the same set of samples, half of them were run first at 5 °C/min and then repeated at 2 °C/min, while the other half underwent the inverse order of heating rates. This approach eliminates the influence of oxidation behaviour from one test to the other. The results are presented as the difference between the temperatures obtained at 2 °C/min and 5 °C/min for possible polymorphic (unknown), eutectic, and liquidus phase transitions.

Generally, it was observed that results obtained at 2 °C/min heating rates were systematically at lower temperatures compared to those at 5 °C/min, for the same phase transition across all samples. However, it was also observed that the DSC signals were not necessarily clearer or easier to interpret at lower heating rates. Nevertheless, results obtained from both heating rates followed the same trend.

For possible polymorphic transitions, it was observed that at $X_{KI} =$ 3.9 mol%, the solid-to-solid phase transition could only be reliably observed at 2 °C/min, while other samples showed mixed results with both positive and negative temperature differences, resulting in an average difference of −0.7 °C (where negative results indicate that 2 °C/min predicts lower off-seat temperatures than at 5 °C/min). For eutectic transitions, despite $X_{KI} = 19.5$ mol% showing the largest difference (-7.6 °C), the average temperature difference was −1.8 °C, following the same trend as the polymorphic transitions. The most significant and consistent difference was observed for the liquidus temperature, where despite X_{KI} = 15.0 mol% showing a small positive difference of 0.7 °C, the average temperature difference for other samples was −5.6 °C, indicating that 2 °C/min heating rate resulted in lower temperatures compared to 5 °C/min.

In terms of the composition difference analysis, increasing the sample composition from 50 mg to 100 mg was intended to minimize possible DSC interpretation errors. However, when comparing DSC signals of samples with similar molar fractions (*e.g.* 55.5, 59.8, and 70.3 mol% of KI), which are similar to 60 mol% of KI (Fig. 3 mol% of KI, which are similar to 86.0 mol% of KI (Fig. 3), it was not possible to conclude that using a sample composition higher than 50 mg was advantageous.

For the KI-CsI system, thermodynamic equilibrium was achieved after the second out of four heating cycles, only for near the eutectic point composition and for an abundance of caution, in total were adopted as transition temperatures varied between the second to the third heating cycle, and no difference was observed on the fourth cycle. The same behaviour was observed for both heating cycle rates and this could be a specific issue related to this system, as it was not observed in the NaI-CsI and NaF-CsI system. However, the authors recommend using four heating cycles for, a heating rate of 5 °C/min, and a sample composition of 50 mg for future studies as it is possible to obtain good DSC signals without too much noise. Heating rates of 2 °C/min should only be used for auxiliary interpretation of 5 °C/min DSC signals, knowing the possibility that liquidus temperatures may be lower than 5 °C/min readings.

Table 7
Final resultant error per system and heating cycle performed at Ontario Tech University. Standard uncertainty was adopted, with 68% confidence interval.

Resultant Error	NaI-CsI [°C]	KI-CsI [°C]	NaF-CsI [°C]	Final [°C]
Eutectic (5 °C/min)	±1.7	± 5.2	±1.7	±5
Eutectic (2 °C/min)	±3.0	± 5.8	±3.0	± 6
Liquidus (5 °C/min)	-	± 9.6	-	± 10
Liquidus (2 °C/min)	-	± 9.9	-	±10

The influence of kinetics and thermal lag from 2 and 5 °C/min was partially investigated using available data for the KI-CsI system, extrapolating them to 0 °C/min. The calculated extrapolated data are presented in Table 6, where the maximum temperature difference between 2 and 5 °C/min was calculated for 0 °C/min, and its average was calculated for the eutectic and liquidus data. These results showed significantly lower temperatures for both transitions and were treated as a direct source of error in Table 4 to minimize impacts due to this phenomenon.

All thermodynamic systems errors (eutectic and liquidus) have been averaged by a simple average of the errors from all systems per heating cycle and final errors are presented in the last column of Table 7. The resulting error of measurements at JRC is ± 5 °C for eutectic and ± 10 °C for liquidus, for both 5 and 10 °C/min. Standard uncertainty was adopted, with 68% confidence interval for JRC's data.

The resultant error of the measurements conducted at Ontario Tech University is ± 0.13% for sample composition. For temperature error, after crossing all main sources of errors related in Table 4, the final resultant temperature uncertainty is ± 5 °C and 6 °C for eutectic and ± 10 °C for liquidus, for both 5 and 2 °C/min, respectively. This error is adopted for all thermodynamic systems investigated and is presented in Table 7.

3. Thermodynamic model development

All thermodynamic models were developed for molten salt and solid solutions if applicable, in addition to stoichiometric compounds, consistent with the JRCMSD, which includes CsI and NaF. For KI and NaI end-members, the studies of Barin et al. [31] were adopted. CsF was included in the JRCMSD to account for its necessity in setting NaF-CsI parameters. The stoichiometric compounds are described in Section 3.1, the model development process is detailed in Section 3.2, the molten salt solution is described in Section 3.3, and the solid solution in Section 3.4.

The general Gibbs energy (G_{sol}) expression for solution phases considered here is:

$$G_{sol} = G^{\circ} + G^{\mathrm{id}} + G^{\mathrm{ex}}, \tag{2}$$

where G° is the weighted sum of the reference Gibbs energy of its species, $G^{\mathrm{id}} = -TS^{id}$ is the ideal Gibbs energy of mixing term, and G^{ex} is an excess term to account for non-ideal mixing.

Table 8
The $\Delta_f H^\circ$ (kJ/mol), S° (J/K mol) and C_p (J/K mol) data of pure compounds used in this study.

Comp.	$\Delta_f H^\circ$	S°	$C_p = a + bT + cT^2 + dT^{-2}$				Temp Range	Ref
	kJ/mol	J/molK	a	b	c	d	[K]	
CsI(s)	−348.10	122.20	43.815	2.184E-02	2.496E-06	2.002E + 05	298–6000	[32,34]
CsI(l)	−331.91	131.89	74.268	-	-	-	298–2500	[32,34]
KI(s_1)	−327.90	106.40	38.836	2.820E-02	-	4.929E + 05	298–2000	[31]
KI(s_2)	−312.90	106.40	38.926	2.820E-02	-	4.929E + 05	298–2000	[31]
KI(l)	−297.86	114.08	72.383	-	-	-	298–2000	[31]
NaI(s)	−287.86	98.32	48.877	1.205E-02	-	-	298–1577	[31]
NaI(l)	−269.69	113.04	64.852	-	-	-	298–1577	[31]
NaF(s)	−576.65	51.21	47.630	1.479E-02	-	−4.643E + 05	298–2500	[33]
NaF(l)	−557.73	52.75	72.989	-	-	-	298–6000	[33]
CsF(s)	−554.67	93.60	24.291	6.461E-02	-	5.900E + 05	298–6000	[3,34]
CsF(l)	−534.71	108.19	70.560	-	-	-	298–6000	[3,34]

3.1. Pure compounds

The Gibbs energy of pure compounds is represented by

$$G(T) = \Delta_f H^\circ(298.15K) + \int_{298.15}^{T} C_p(T)dt - T\cdot\left(S^\circ(298.15K) + \int_{298.15}^{T}\frac{C_p(T)}{T}dT\right) \quad (3)$$

in which T is the absolute temperature, S^0 $(298.15K)$ is the standard absolute entropy, ΔfH^0 $(298.15K)$ is the standard enthalpy of formation, and $C_p(T)$ is the heat capacity at constant pressure as a function of the temperature, represented by

$$C_p(T) = a + bT + cT^2 + dT^{-2} \quad (4)$$

where the variables $a-d$ are empirical coefficients [3,31–34]. All functions can be found in Table 8.

3.2. Model development process for liquid and solid solutions

Interaction parameters for the molten salt solutions and solid solutions were calculated using multiple methods, including Optima [35] and OptiSage 7.1 (available in FactSage 8.0). The final parameters were determined based on a combination of the experimental values obtained in this study and other available results in the open literature with different weighting factors depending on the intended interpretation by the authors for each thermodynamic system.

3.3. Liquid solutions

The Modified Quasichemical Model in the Quadruplet Approximation (MQMQA) [36–40] has been used in this work to be consistent with the JRCMSD. A description of the model including derivations of the chemical potential expression is given by Poschmann et al. [41]. The purpose of the MQMQA is to account for the effects of Short-Range Order (SRO) of both First-Nearest-Neighbors (FNN) and Second-Nearest-Neighbors (SNN) in liquid solutions by considering SNN quadruplets [39]. This model allows for the incorporation of short-range ordering, including interactions between first-nearest neighbours and second-nearest neighbours, in a two-sublattice phase for the NaI-CsI and KI-CsI systems. In these systems, the second sublattice consists of only a single anion, iodine, while the first sublattice contains sodium or potassium as cations. On the other hand, in the NaF-CsI system, the second sublattice contains two anions, fluorine and iodine, in addition to the two cations, Na and Cs.

In single-anion systems, the excess parameter for the Gibbs energy is represented as $\Delta g_{AB/I}$ for the SNN pair exchange reaction on a quasi-lattice. For the KI-CsI and NaI-CsI systems, iodine is the only anion in the mixture. Therefore, no excess Gibbs energy is associated with the anion-anion interaction. A and B represent two of the cations (K, Cs or Na). In this way, the formation of the second nearest neighbour pair A-I-B is represented by Eq. 5.

$$\left(A-I-A\right) + \left(B-I-B\right) = 2\left(A-I-B\right) \qquad \Delta g_{AB/I} \quad (5)$$

where $\Delta g_{AB/I}$ is the Gibbs energy change related to the pair formation. This is an empirical parameter model and is represented in polynomial form as written by Eq. 6:

$$\Delta g_{AB/I} = \Delta g_{AB/I}{}^\circ + \sum_{i>1} g^{i0}_{AB/I}x^i_{AB/I} + \sum_{j>1} g^{0j}_{AB/I}x^j_{BA/I} \quad \left[J\Big/mol\right] \quad (6)$$

where $\Delta g^0_{AB/I}$ and $g^{ij}_{AB/I}$ are composition-independent coefficients while the dependence on composition is given by the $x_{AB/I}$ terms, defined as a function of the cation-cation pair mole fractions x_{AA}, x_{BB}, and x_{AB}. The resulting parameters were optimized in this work and are given below:

$$\Delta g_{KCs/I} = -1143.48 + x_{KCs/I}\left(5182.539 - 5.48T\right) + x_{CsK/I}\left(7909.40 - 14.32T\right) \quad \left[J\Big/mol\right] \quad (7)$$

$$\Delta g_{NaCs/I} = -2347.56 + x_{NaCs/I}\left(-1493.54 + 4.03T\right) + x_{CsNa/I}\left(5182.539 - 5.48T\right) \quad \left[J\Big/mol\right] \quad (8)$$

In this work, the reciprocal salt system (NaF-CsI) presents a second anion (fluorine) on sublattice II. A more detailed description of the thermodynamic model involving reciprocal salts, including generic quadruplets AB/I_2, A_2/IF and AB/IF for these systems, can be found in Capelli et al. [5]. The excess Gibbs energy for the NaF-CsI (Cs;Na//I,F) salt can be expressed by Eq. 9 and 10:

$$\Delta g_{CsNa/IF} = -1979.63 - 12438.66\cdot x_{CsI} \quad \left[J\Big/mol\right] \quad (9)$$

$$\Delta g_{CsNa/IF} = 1000 - 20000\cdot x_{CsI} + 20000\cdot x_{NaF} \quad \left[J\Big/mol\right] \quad (10)$$

3.4. Solid solution

The excess Gibbs energy function of the solid solutions is only formed in the KI-CsI binary system and is presented as a substitutional solution model, which is based on the assumption that the constituents mix randomly on a single lattice [42]. The Kohler-Toop interpolation method was adopted, which is an asymmetrical model that is used when one species of the subsystem belongs to a group different from the others [43]. Detailed information can be found in Bajpai et al. [44]. Thus, the excess Gibbs energy is represented by Eq. 11.

$$\Delta g_{(K,Cs)I} = 14064.62\cdot x_{KI} + 7708.66\cdot x_{CsI} \quad \left[J\Big/mol\right] \quad (11)$$

Table 9
NaI-CsI Samples and phase transitions results. [a] Sample mass of 50 mg.

X_{NaI}	Heating Rate	Phase Transition	T [°C]	Phase Transition	T [°C]
0.000[a]	5 °C/min	-		Liquidus	627.1
0.213[a]	5 °C/min	Eutectic	431.6	Liquidus	569.8
0.399[a]	5 °C/min	Eutectic	432.0	Liquidus	480.4
0.528[a]	2 °C/min	Eutectic	431.8	Liquidus	462.1
0.602[a]	5 °C/min	Eutectic	432.0	Liquidus	506.8
0.799[a]	5 °C/min	Eutectic	432.4	Liquidus	594.8
1.000[a]	5 °C/min	-		Liquidus	657.9

* Internal pressures within the hermetically sealed SS crucibles were not monitored but showed no influence on pure component's melting temperature for up to 3.65 atm at 800 °C. NaI-CsI presented temperature uncertainty, $u(T) = \pm 5$ °C and ± 6 °C for eutectic, and ± 10 °C and ± 10 °C for liquidus, for at 5 and 2 °C/min, respectively, for 0.68 level of confidence. Mixture uncertainty was evaluated to be $u(x_{i-j}) = \pm 0.13$ mol% for the same standard uncertainty.

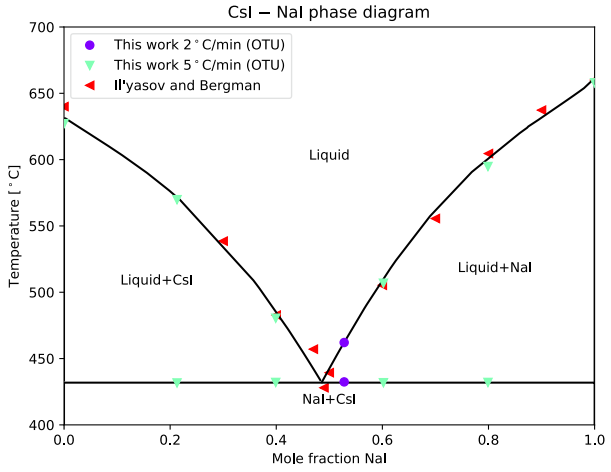

Fig. 2. NaI-CsI phase diagram proposed by the present work. Experimental data points used for comparison from Il'yasov and Bergman [13] are available in the Appendix. NaI + CsI solid phase has not been validated by XRD measurements, but follows interpretation from Il'yasov and Bergman [13].

4. Results and Discussion

Results of single components measurements are described in §4.1, whereas the NaI-CsI, KI-CsI and NaF-CsI systems are presented in §4.2, §4.3 and §4.4, respectively. A detailed error analysis was presented in §2.5.

4.1. Single Component Measurements

Prior to any mixtures being analyzed, the purity of individual components in each system was confirmed by DSC melting point measurements, which were compared to accepted values reported in the literature. The obtained melting point measurements in this work are in good agreement with literature values and the safety data sheet provided by Sigma–Aldrich (99.99% trace metals basis), with NaI (657.9 °C against 661 °C [20]), CsI (631.5 °C against 626.0 °C [21,45]), KI (679.0 °C against 682.0 °C [22]), and NaF (997.4 °C against 993.0 °C [23]). The general error for pure components at Ontario Tech University is ± 6 °C, and ± 5°C for measurements performed at JRC. More details about the error analysis can be found in §2.5.

4.2. The NaI-CsI system

Sangster [14] highlighted large uncertainties in different regions of the CsI-NaI phase diagram (*i.e.*, 80 °C) and good agreement in others (*i.e.*, 1 °C) [12,13]. The study of Il'yasov and Bergman [13] was therefore taken as a guide for developing a thermodynamic model as the maximum described inaccuracy was ± 20 °C.

Due to the reported uncertainty associated with the liquidus and eutectic point from previous studies, five mixture samples for the NaI-CsI system were measured in this work. As shown in Table 9, only one point close to the eutectic point was measured at a heating rate of 2 °C/min to achieve better precision, whereas other compositions were added at 5 °C/min.

The CsI melting point in this work was found to be lower at 631.5 °C compared to the value reported by Il'yasov and Bergman [13], which was 639.5 °C, but is closer agreement to standard values in the literature (632.0 ± 2 °C [45]). The only noticeable difference was at the eutectic line, which was found to be 4.7 °C higher at 432.5 °C in this work, compared to 427.8 °C reported in Il'yasov and Bergman [13]. The results of all phase transitions are summarized in Table 9, and the thermodynamic model with the experimental comparison between available results is illustrated in Fig. 2. The phase diagram of this and subsequent thermodynamic systems was generated by Thermochimica [41,46] using a new module for creating diagrams.

4.3. The KI-CsI system

A total of seventeen DSC measurements were performed on the KI-CsI system by OTU. Table 10 summarizes additional details such as sample masses, ranging from 50 mg to 100 mg. Samples near the eutectic points used a heating rate of 2 °C/min to better analyze phase-transition signals, while others used 5 °C/min. Due to the complexity of this system and the potential for different interpretations, three additional samples were performed by JRC to corroborate measurements. DSC measurements of the KI-CsI system were conducted in a virtually identical manner to those of the NaI-CsI system. The DSC signals of several samples of the KI-CsI system are illustrated in Fig. 3.

The liquidus of the KI-CsI system was previously reported by Samuseva and Plyushchev [15] (± 40 °C) and Sato et al. [17] (± 1 °C). However, liquidus temperatures from Samuseva and Plyushchev [15] are significantly distinct from results observed by OTU, JRC and Sato [17], illustrated in Fig. 4.

The study by Samuseva and Plyushchev [15] measured the eutectic point as 536 °C at 39.0 mol% of KI, but with a significant uncertainty ranging between ± 40 to 65 °C [15]. In contrast, the study by Sato et al. [17] identified the eutectic point at 555 °C ± 1 °C at 38.6 mol% of KI, which is in clear agreement with the measured eutectic point obtained in the present study (555 °C ± 1.7 °C at 39.0 mol% of KI). The samples developed in this study aimed to identify if possible polymorphic phases and solvus transition are consistent and easy to detect solely using DSC.

A possible polymorphic transitions or a displaced eutectic phase transition were difficult to interpret from points $X_{KI} = 11.0$, 19.5, 27.0, and 48.5 mol%. Among these, only the sample with $X_{KI} = 19.5$ mol% clearly showed an onset temperature at 540 °C, eutectic and liquidus temperature. In addition, this possible polymorphic transition was not consistently observed in the adjacent samples, with X_{KI} 15.0 and 23.4 mol%. In the study of Sato [17], no possible polymorphic transitions were observed. However, Samuseva and Plyushchev [15] showed several points around 525 °C, but with large inconsistencies to one another. For the development of the thermodynamic model of this system, this possible polymorphic transition was not assumed due to the absence of convincing experimental data. Results obtained using a heating rate of 2 °C/min was adopted, whenever available, otherwise 5 °C/min signals were used (Table 10).

Previous studies [15,16,47] investigated the evidence of solid solubility in the KI-CsI system but no clear evidence was found. Sangster

Table 10
KI-CsI Samples and phase transitions. [a] Sample mass of 50 mg, [b] Sample mass of 100 mg, [*] Measurements made from JRC. [c] Polymorphic was not detectable through DSC signals and was not validated by XRD. Heating rate units in °C/min.

X_{KI}	Heating Rate	Transition	T [°C]	Transition	T [°C]	Transition	T [°C]
0.039 [a]	2	Solvus	316.3	Solidus	608.1	Liquidus	621.4
0.039 [a]	5	Solvus	310.0	Solidus	610.1	Liquidus	628.4
0.070 [b]	2			Solidus	600.0	Liquidus	616.6
0.070 [b]	5			Solidus	599.9	Liquidus	622.0
0.110 [b]	2	Polymorphic [c]	539.7			Liquidus	606.0
0.110 [b]	5	Polymorphic [c]	540.4			Liquidus	610.9
0.150 [b]	2			Eutectic	553.6	Liquidus	608.1
0.150 [b]	5			Eutectic	553.6	Liquidus	607.4
0.195 [b]	2	Polymorphic [c]	538.2	Eutectic	553.6	Liquidus	589.3
0.195 [b]	5	Polymorphic [c]	540.2	Eutectic	561.2	Liquidus	596.2
0.234 [b]	2			Eutectic	553.5	Liquidus	579.2
0.270 [b]	2	Polymorphic [c]	539.1			Liquidus	559.8
0.270 [b]	5	Polymorphic [c]	538.3			Liquidus	564.6
0.309 [b]	2			Eutectic	553.9	Liquidus	562.3
0.309 [b]	5			Eutectic	554.6	Liquidus	567.3
0.347 [a]	2			Eutectic	555.8	Liquidus	561.5
0.442 [b]	2			Eutectic	554.9	Liquidus	564.7
0.485 [b]	2	Polymorphic [c]	539.8			Liquidus	568.1
0.555 [b]	5			Eutectic	557.7	Liquidus	581.7
0.598 [a]	5			Eutectic	559.0	Liquidus	588.8
0.703 [b]	2			Eutectic	558.7	Liquidus	613.5
0.703 [b]	5			Eutectic	559.5	Liquidus	618.6
0.800 [a]	2			Solidus	576.4	Liquidus	638.2
0.861 [a]	2			Solidus	623.7	Liquidus	648.1
0.951 [a]	2			Solidus	656.8	Liquidus	671.2
0.951 [a]	5			Solidus	658.1	Liquidus	676.6
1.000 [a]	2					Liquidus	679.0
1.000 [a]	5					Liquidus	680.2
1.000 [b]	5					Liquidus	684.2
0.200 [a*]	5			Eutectic	557.7	Liquidus	591.1
0.200 [a*]	10			Eutectic	557.7	Liquidus	591.1
0.310 [a*]	5			Eutectic	559.0		
0.310 [a*]	10			Eutectic	559.0		
0.800 [a*]	5			Eutectic	572.3	Liquidus	639.6
0.800 [a*]	10			Eutectic	572.3	Liquidus	639.6

* Internal pressures within the hermetically sealed SS crucibles were not monitored but showed no influence on pure component's melting temperature for up to 3.21 atm at 680.2 °C. KI-CsI presented temperature uncertainty $u(T) = \pm 5$ °C and ± 6 °C for eutectic, solvus and solidus, and ± 10 °C and ± 10 °C for liquidus, for at 5 and 2 °C/min, respectively. Mixture uncertainty was evaluated to be $u(x_{i-j}) = \pm 0.13$ mol% for the same standard uncertainty. Standard uncertainty (u) was calculated for a 0.68 level of confidence.

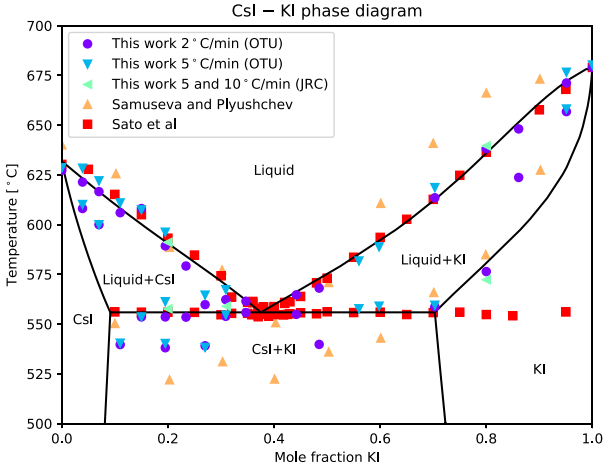

Fig. 4. KI-CsI phase diagram proposed. Plotted for a temperature range between 500 to 700 °C. Experimental points used for comparison from Samuseva and Plyushchev [15] and Sato et al. [17] are available in the Appendix. CsI, CsI + KI and KI solid phases have not been validated by XRD measurements, but follow interpretation from Samuseva and Plyushchev [15].

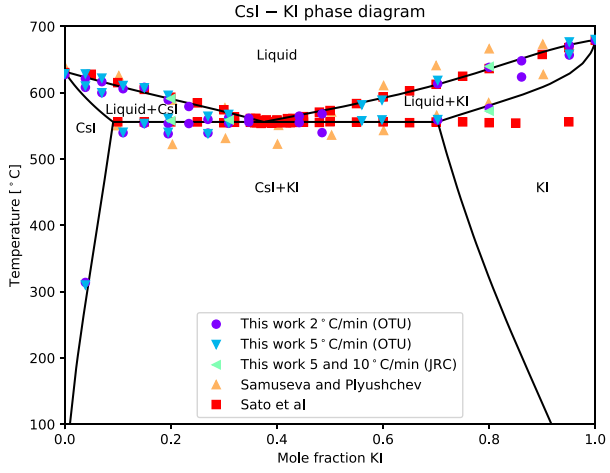

Fig. 5. KI-CsI phase diagram proposed. Plotted for a temperature range between 100 to 700 °C. Experimental points used for comparison from Samuseva and Plyushchev [15] and Sato et al. [17] are available in the Appendix. CsI, CsI + KI and KI solid phases have not been validated by XRD measurements, but follow interpretation from Samuseva and Plyushchev [15].

Table 11
NaF-CsI Samples and phase transitions. [a] Sample mass of 50 mg. * performed by JRC. Heating rate unit in °C/min.

X_{CsI}	Heating Rate	Phase Transition	Transition [°C]	Phase Transition	Transition [°C]
1.000 [a]	5			Liquidus	627.1
0.955 [a]	2	Eutectic	611.9	Liquidus	618.7
0.955 [a]	5	Eutectic	611.9	Liquidus	624.0
0.900 [a]	2	Eutectic	611.9	Liquidus	660.7
0.900 [a]	5	Eutectic	611.6	Liquidus	N/A
0.858 [a]	2	Eutectic	613.6	Liquidus	805.0
0.858 [a]	5	Eutectic	612.2	Liquidus	N/A
0.800 [a]	5	Eutectic	614.3	Liquidus	871.6
0.600 [a]	5	Eutectic	614.7	Monotectic	946.9
0.400 [a]	5	Eutectic	614.7	Monotectic	963.3
0.200 [a]	5	Eutectic	614.5	Monotectic	955.0
0.000 [a]	5			Liquidus	997.4
0.500 [a*]	5	Eutectic	611.6	Monotectic	959.5
0.300 [a*]	5	Eutectic	611.4	Monotectic	975.6
0.100 [a*]	5	Eutectic	606.6	Monotectic	978.1

* Internal pressures within the hermetically sealed SS crucibles were not monitored but showed no influence on pure component's melting temperature for up to 5.33 atm at 1250 °C. NaF-CsI presented temperature uncertainty of ± 5 °C and ± 6 °C for eutectic, and ± 10 °C and ± 10 °C for liquidus and monotectic, for at 5 and 2 °C/min, respectively. Mixture uncertainty was evaluated to be ± 0.13 mol%. Standard uncertainty (u) was calculated for a 0.68 level of confidence.

[14] did consider the possible solid solubility data from Samuseva's [15] experimental data despite the question of the nature of the solid state of this system remaining unresolved. Sato et al. [17] could also not identify the solid solution phase KI using TG-DTA measurements. To obey the Gibbs phase rule, and be consistent with the current proposed solvus line on the rich KI side, at 80% mol of KI, at approximately 575 °C, the study preferred to maintain the previous interpretation of Sangster [14] regarding the solid solution phase KI.

In this work, the solubility of solid solution phases was assumed to be between 7.0 mol% and 65.0 mol% of KI, as reported in Sangster's model [14] and Samuseva's experimental results [15]. In contrast, the latter work of Sato et al. [17] observed different signals, where complete immiscibility was found. Fig. 4 provides a comparison of both sets of results in addition to this work.

A clear signal of solid solubility was identified at 3.9 mol% of KI, at 313.9 °C, indicating limited solid solubility of KI into CsI. However, it is unknown why the solvus between CsI + KI to CsI and KI was not detected at 7% and 70% of KI, respectively, which limited confidence regarding the solvus transition observed at 3.9 mol% of KI. Nevertheless, solvus from CsI + KI to pure CsI and pure KI have been assumed based on previous interpretations of Samuseva and Plyushchev [15]. On the other hand, OTU's (80.0 and 86.0 mol% of KI) and JRC's (80.0 mol% of KI) samples were not able to observe an indication of an extended solid solution phase rich in KI. However, higher onset temperatures were observed at 638.2 °C (OTU) and 639.6 °C (JRC) for 80 mol% of KI. This artifact coupled with the Gibbs phase rule, raises the necessity of an extended solid solution phase rich in KI. For this reason, the KI solvus line was adopted in this study (Figs. 4 and 5), but further experiments using different techniques (*i.e.*, X-ray Diffraction (XRD)) may be needed in future studies to confirm this solid solution phase.

The proposed thermodynamic model for this system is somewhat similar to the one proposed by Samuseva [15], with adjustments made based on the current results. However, the eutectic temperature from Sato et al. [17] was maintained in the model due to several samples supporting this interpretation. The possible polymorphic phase observed at approximately 540 °C in this work was completely neglected in the model due to the lack of consistency in the experimental results.

4.4. The NaF-CsI System

No available data was found for the NaF-CsI system in the literature. In the present study, the eutectic point was measured to be ≈93 mol% CsI at 614 °C. It was not possible to observe liquidus temperatures for 90.0 and 85.8 mol% CsI mixtures using a heating rate of 5 °C/min, only at 2 °C/min. Three additional measurements were performed at JRC to

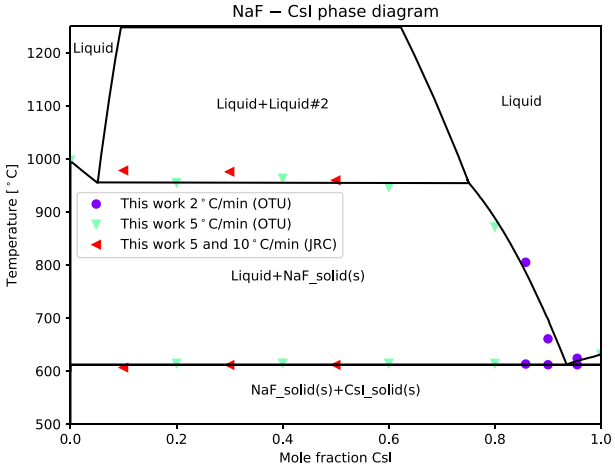

Fig. 6. NaF-CsI phase diagram with experimental data-points from this work. NaF + CsI solid phase has not been validated by XRD measurements and it was assumed based on DSC measurements. Liquid 1 + Liquid 2 miscibility gap has not been validated.

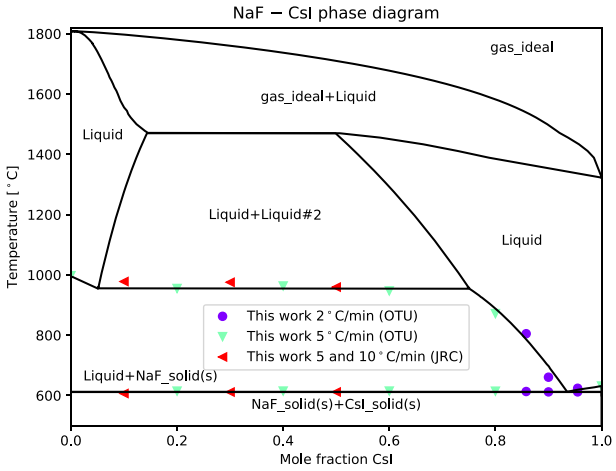

Fig. 7. NaF-CsI phase diagram with experimental data points from this work with detail for gaseous phase. NaF + CsI, Liquid 1 + Liquid 2 and gaseous-containig regions have not been validated.

Table 12
NaI-CsI data*, obtained from the study of Il'yasov and Bergman [13].

X_{NaI}	Temp [°C]	X_{NaI}	Temp [°C]
0.000	640.0	0.600	505.3
0.300	538.6	0.700	555.6
0.400	482.8	0.800	604.6
0.470	457.1	0.900	637.3
0.490	428.0	1.000	660.0
0.500	439.4		

*Temperature uncertainty of ± 20 °C [13] treated with standard uncertainty (u) of 0.68 level of confidence. There is no available data regarding mixture composition and internal pressure uncertainties.

Table 13
KI-CsI data*, obtained from Sato et al. [17].

X_{KI}	Temp [°C]	X_{KI}	Temp [°C]	X_{KI}	Temp [°C]	X_{KI}	Temp [°C]
0.000	630.3	0.360	561.4	0.401	554.9	0.650	554.8
0.050	627.8	0.360	560.7	0.418	554.6	0.650	602.7
0.100	556.1	0.362	554.9	0.420	560.9	0.700	555.8
0.100	615.2	0.370	553.7	0.420	560.4	0.700	612.7
0.150	556.0	0.370	556.2	0.425	554.9	0.750	556.0
0.150	605.0	0.370	557.9	0.430	555.2	0.750	624.8
0.200	556.0	0.376	555.3	0.430	561.2	0.800	554.8
0.200	593.2	0.380	554.9	0.450	555.7	0.800	636.4
0.250	555.9	0.380	558.7	0.450	563.9	0.850	554.2
0.250	584.7	0.380	557.9	0.480	555.2	0.900	553.5
0.300	554.7	0.380	558.6	0.480	570.7	0.900	657.7
0.300	574.3	0.386	555.4	0.500	556.2	0.950	556.1
0.320	555.4	0.390	554.0	0.500	573.1	0.950	668.0
0.320	563.6	0.390	556.0	0.550	555.8	1.000	679.0
0.350	555.4	0.400	554.8	0.550	583.6		
0.350	561.1	0.400	558.4	0.600	556.0		
0.358	554.7	0.400	558.8	0.600	593.6		

*Temperature uncertainty of ± 1 °C and composition uncertainty of 0.1 mol% [17] treated with standard uncertainty (u) of 0.68 level of confidence. There is no available data regarding internal pressure uncertainty.

investigate a possible miscibility gap between 10 to 50 mol% CsI. This was made because a slight noise was observed at 1050 °C by OTU's samples. Additional samples made by JRC (10, 30 and 50 mol% CsI) were heated up to 1200 °C, respecting the temperature limitation to avoid salt boiling, but no signals of a miscibility gap were found for these samples. Results obtained by both OTU and JRC are summarized in Table 11.

While DSC signals did not indicate miscibility gaps for this system, they have been identified in different thermodynamic studies involving reciprocal salts, such as in the LiF-CsI and ThF_4-CsI systems explored by Capelli et al. [5]. A comprehensive analysis revealed that omitting a miscibility gap from the model made it difficult to align the model with experimental data. To accommodate the observed temperature plateau between 10% CsI to 60% CsI, recognizing a miscibility gap proved to yield a suitable fit to the current experimental data. The proposed phase diagram is presented in Fig. 6.

The proposed miscibility gap is postulated to extend to higher temperatures than what was measured in this campaign. To depict its potential influence on the boiling point, this model is extrapolated to 1800 °C in Fig. 7. Experimental measurements of these phase transitions is needed to validate the phase diagram at higher temperatures, which is beyond the max use temperature of the current procedure of approximately 1200 °C. Future experiments are recommended to corroborate the suggested miscibility gap by utilizing techniques such as quenching samples and subsequent analysis using scanning electron microscopy and energy-dispersive X-ray spectroscopy. Future DSC experiments at higher temperatures should consider the possibility of preferential volatilization affecting composition.

Table 14
KI-CsI data*, obtained from Samuseva and Plyushchev [15].

X_{KI}	Temp [°C]	X_{KI}	Temp [°C]	X_{KI}	Temp [°C]	X_{KI}	Temp [°C]
0.000	640.1	0.302	577.2	0.503	570.9	0.799	584.9
0.100	550.3	0.303	531.1	0.601	543.0	0.800	666.2
0.102	625.6	0.401	522.4	0.601	610.7	0.901	673.2
0.203	522.0	0.403	550.7	0.700	640.9	0.902	627.4
0.203	588.6	0.503	536.0	0.701	565.9	1.000	680.4

*Temperature uncertainty of ± 40 °C [15] treated with standard uncertainty (u) of 0.68 level of confidence. There is no available data regarding mixture composition and internal pressure uncertainties.

5. Conclusions

This study has contributed to the further understanding of the NaI-CsI, KI-CsI, and NaF-CsI pseudo-binary systems by, providing new experimental data:

- The liquidus obtained for the NaI-CsI system was in good agreement with previous studies, which used TG-DTA analysis, but this time, the eutectic was able to be observed using DSC technique. An excellent fit between experimental results and the thermodynamic model is provided.
- For the KI-CsI system, divergent results from previous studies were clarified, some knowledge gaps were filled on CsI solid solution and the eutectic point and confidence were gained in the system as a whole. However, there are still uncertainties with this system, especially for the possible solid solubility where KI is rich (>70% mol of KI-CsI), where CsI is rich (<9% mol of KI-CsI) and possible polymorphic phase transitions between 520–540 °C. A thermodynamic model is provided taking into consideration contributions from previous work, but differences were solved using the present experimental data.
- The NaF-CsI system was experimentally investigated for the first time, and consistent experimental results between OTU and JRC's samples were obtained. The thermodynamic modelling of reciprocal salts was challenging and further investigation is needed for this type of system.
- For all systems, the use of 50 mg samples at 5 °C/min obtained good DSC signals. However, it was noticed that for most of the 2 °C/min measurements of the KI-CsI system, liquidus temperatures presented noticeably lower results, but within final error uncertainty. The usage of 2 °C/min heating rate should be used with the auxiliary intention of better interpreting 5 °C/min signals. At the same time, no significant improvement was observed when increasing sample composition masses.

All pseudo-binary systems were developed to directly support the development of the JRCMSD and contribute to the understanding of the solubility behaviour of CsI, NaI, KI, and NaF in molten salt systems.

6. Recommended Future Work

The authors would like to suggest future work for the following systems, as not all knowledge gaps could be filled using exclusively DSC.

KI-CsI: Heating 4–96, 70–30, and 90–10 mol% KI-CsI samples to 500 °C, quenching the sample, and post-analysis using XRD, Scanning electron microscopy (SEM) and/or Energy Dispersive X-ray spectroscopy (EDS) to differentiate crystal structures. This would help better understand the solvus phase transition. Heating 20–80, 40–60, 60–40 mol% KI-CsI samples to 550°C and repeat the same process, to identify if a possible polymorphic phase transition exists.

CsI-NaF: Heating 20–80 and 40–60 mol% CsI-NaF for up to 1200 °C, quenching the sample, and post-analyzing it using SEM/EDS analysis to

investigate the miscibility gap between Liquid 1 and Liquid 2. The same could be done for 5–95, 80–20 and 90–10 mol% CsI-NaF to analyze if only Liquid 1 is present.

CRediT author statement

N. L. Scuro: DSC measurements of NaI-CsI and KI-CsI system, DSC analysis, model development, figures, writing, editing. **B.W.N. Fitzpatrick**: DSC measurements of NaF-CsI, and DSC analysis. **E. Geiger**: DSC measurements of NaF-CsI and DSC analysis. **M. Poschmann**: model development, writing, Thermochimica GUI phase diagram implementation. **O. Beneš and T. Dumaire**: DSC corroborative measurements of KI-CsI and NaF-CsF, writing, review. **M.H.A. Piro**: conceptualization, writing, editing, revision.

Declaration of Competing Interest

The authors declare the following financial interests/personal relationships which may be considered as potential competing interests: Nikolas Lymberis Scuro reports financial support was provided by Ontario Tech University.

Data availability

The authors do not have permission to share data.

Acknowledgements

This research was undertaken, in part, thanks to funding from the Canada Research Chairs program of the Natural Sciences and Engineering Research Council of Canada, grant # 950–231328. Funding for equipment from the Canadian Foundation for Innovation, grant # 35712, the Ontario Ministry of Economic Development, Job Creation Trade, grant # 35712 is greatly acknowledged.

Appendix A

Additional data from the NaI-CsI system were obtained from the study of Il'yasov and Bergman [13], described in Table 12.

Additional data from the KI-CsI system were obtained from the study of Sato et al. [17], described in Table 13. From the same system, additional data from Samuseva and Plyushchev [15] was used for comparison, represented in Table 14.

References

[1] J. Serp, M. Allibert, O. Beneš, S. Delpech, O. Feynberg, V. Ghetta, D. Heuer, D. Holcomb, V. Ignatiev, J.L. Kloosterman, et al., The molten salt reactor (MSR) in generation IV: Overview and perspectives, Prog. Nucl. Energy 77 (2014) 308–319.
[2] O. Beneš, M. Beilmann, R. Konings, Thermodynamic assessment of the LiF-NaF-ThF_4-UF_4 system, J. Nucl. Mater. 405 (2010) 186–198.
[3] O. Beneš, R. Konings, D. Sedmidubskỳ, M. Beilmann, O. Valu, E. Capelli, M. Salanne, S. Nichenko, A comprehensive study of the heat capacity of CsF from T= 5 K to T= 1400 K, J. Chem. Thermodyn. 57 (2013) 92–100.
[4] J. Ocadiz-Flores, E. Capelli, P. Raison, R. Konings, A. Smith, Thermodynamic assessment of the LiF-NiF_2, NaF-NiF_2 and KF-NiF_2 systems, J. Chem. Thermodyn. 121 (2018) 17–26.
[5] E. Capelli, O. Beneš, R. Konings, Thermodynamics of soluble fission products cesium and iodine in the molten salt reactor, J. Nucl. Mater. 501 (2018) 238–252.
[6] J.A. Ocádiz-Flores, E. Carré, J.-C. Griveau, E. Colineau, E. Capelli, P. Souček, O. Beneš, R. Konings, A. Smith, Thermodynamic assessment of the KF-ThF_4, LiF-KF-ThF_4 and NaF-KF-ThF_4 systems, J. Chem. Thermodyn. 145 (2020) 106069.
[7] O. Beneš, P. Soucek, Molten salt reactor fuels, in: M.H.A. Piro (Ed.), Advances in Nuclear Fuel Chemistry, Elsevier, Oxford, 2020.
[8] F. Gelbard, B.A. Beeny, L.L. Humphries, K.C. Wagner, L.I. Albright, M. Poschmann, M.H. Piro, Application of MELCOR for Simulating Molten Salt Reactor Accident Source Terms, Nucl. Sci. Eng. 197 (10) (2023) 2723–2741.
[9] E.C. Beahm, Y.-M. Wang, S.J. Wisbey, W.E. Shockley, Organic iodide formation during severe accidents in light water nuclear reactors, Nucl. Technol. 78 (1) (1987) 34–42.
[10] L. Bosland, F. Funke, G. Langrock, N. Girault, Paris project: Radiolytic oxidation of molecular iodine in containment during a nuclear reactor severe accident: Part 2. formation and destruction of iodine oxides compounds under irradiation – experimental results modelling, Nucl. Eng. Des. 241 (9) (2011) 4026–4044.
[11] E.C. Joint Research Centre, "Joint Research Centre Molten Salt Database (JRCMSD) - Thermodynamic Database on Molten Salt Reactor Systems.".
[12] R. Samuseva, V. Plyushchev, Fusion in Binary systems of caesium and sodium halides, Russ. J. Inorg. Chem. 6 (1961) 1092–1094.
[13] I. Il'yasov, A. Bergman, Ternary reciprocal systems of cadmium, caesium, potassium and sodium halides, Russ. J. Inorg. Chem. 9 (1964) 768–771.
[14] J. Sangster, A.D. Pelton, Phase diagrams and thermodynamic properties of the 70 binary alkali halide systems having common ions, J. Phys. Chem. Ref. Data 16 (3) (1987) 509–561.
[15] R.G. Samuseva, V.E. Plyushchev, The KI-RbI, CsI-KI, CsI-RbI Systems, Russ. J. Inorg. Chem. 9 (10) (1964) 1313–1315.
[16] I.I. Il'yasov and A.G. Bergman Russian Journal of Inorganic Chemistry, vol. 10, no. 681, 1965.
[17] T. Sato, S. Toda, T. Tachikawa, Phase Diagrams of the NaI-KI and KI-CsI Binary Systems, Denki Kagaku oyobi Kogyo Butsuri Kagaku 55 (8) (1987) 617–620.
[18] I.I. Il'yasov, N.I. Chaurski, D.G. Barsegov, Russ. J. Inorg. Chem. 11 (1966) 1984.
[19] K. Lipkina, K. Palinka, E. Geiger, B. Fitzpatrick, O. Välu, O. Beneš, M. Piro, Thermodynamic investigations of the LiF-CsF and NaF-CsF pseudo-binary systems, J. Nucl. Mater. 568 (2022) 153901.
[20] "Material Safety Data Sheet - Sodium iodine (99.999% trace metals basis) - CAS-No. 7681-82-5," Sigma-Aldrich, Oakville, Ontario, 2021.
[21] "Material Safety Data Sheet - Cesium Iodine (99.999% trace metals basis) - CAS-No. 7789-17-5," Sigma-Aldrich, Oakville, Ontario, 2020.
[22] "Material Safety Data Sheet - Potassium iodine (99.999% trace metals basis) - CAS-No. 7681-11-0," Sigma-Aldrich, Oakville, Ontario, 2021.
[23] "Material Safety Data Sheet - Sodium Fluoride (99.99% trace metals basis) - CAS-No. 7681-49-4," Sigma-Aldrich, Oakville, Ontario, 2021.
[24] M. Piro, K. Lipkina, D. Hallatt, Exploring crucible designs for differential scanning calorimetry measurements of fluoride salts, Thermochim. Acta 699 (2021) 178860.
[25] O. Beneš, R. Konings, S. Wurzer, M. Sierig, A. Dockendorf, A DSC study of the $NaNO_3$–KNO_3 system using an innovative encapsulation technique, Thermochim. Acta 509 (1) (2010) 62–66.
[26] Netzsch-Gerätebau GmbHF, "Netzsch Proteus®-Thermal Analysis Software (Software Version 6.1.0)", 2018.
[27] E. Charsley, C. Earnest, P. Gallagher, M. Richardson, Preliminary round-robin studies on the ICTAC certified reference materials for DTA: barium carbonate and strontium carbonate, J. Therm. Anal. Calorim. 40 (3) (1993) 1415–1422.
[28] G.J. Janz, J.J. Slowick, Investigations of CsCl, K_2SO_4, and K_2CrO_4 as high temperature calibrants for differential scanning calorimetry, Zeitschrift für anorganische und allgemeine Chemie 586 (1) (1990) 166–174.
[29] Netzsch Instruments North America, LCC, "Netzsch Analyzing & Testing Business Unit, Temperature and Sensitivity Calibration Protocol, Software Manual DSC Instruments, Technical Document," 2012.
[30] K. Lipkina, Experimental investigations of thermodynamic properties of the LiF-CsF binary system and FliNaK (Master' Thesis), Ontario Tech University, Oshawa, Canada, 2020.
[31] I. Barin, O. Knacke, O. Kubaschewski, Thermochemical properties of inorganic substances: supplement, Springer Science & Business Media, 2013.
[32] F.-Z. Roki, M.-N. Ohnet, S. Fillet, C. Chatillon, I. Nuta, Critical assessment of thermodynamic properties of CsI solid, liquid and gas phases, J. Chem. Thermodyn. 70 (2014) 46–72.
[33] O. Beneš, M. Beilmann, R. Konings, Thermodynamic assessment of the LiF-NaF-ThF_4-UF_4 system, Journal of Nuclear materials 405 (2) (2010) 186–198.
[34] E. Capelli, O. Beneš, R. Konings, Thermodynamics of soluble fission products cesium and iodine in the molten salt reactor, J. Nucl. Mater. 501 (2018) 238–252.
[35] M.H.A. Piro, J.S. Bell, M. Poschmann, A. Prudil, and P. Chan, "A Jacobian Free Deterministic Method for Solving Inverse Problems," arXiv, vol. 2203.04138, 2022.
[36] A. Pelton, S. Degterov, G. Eriksson, C. Robelin, Y. Dessureault, The modified quasichemical model I – binary solutions, Metallurgical and Materials Transactions B 31B (2000) 651–659.
[37] A. Pelton, P. Chartrand, The modified quasichemical model II – multicomponent solutions, Metallurgical and Materials Transactions A 32A (2001) 1355–1360.
[38] P. Chartrand, A. Pelton, The modified quasichemical model III – two sublattices, Metallurgical and Materials Transactions A 32 (6) (2001) 1397–1407.
[39] A. Pelton, P. Chartrand, G. Eriksson, The modified quasichemical model IV – two-sublattice quadruplet approximation, Metallurgical and Materials Transactions A 32A (2001) 1409–1416.

[40] G. Lambotte, P. Chartrand, Thermodynamic evaluation and optimization of the Al_2O_3–SiO_2–AlF_3–SiF_4 reciprocal system using the modified quasichemical model, J. Am. Ceram. Soc. 94 (11) (2011) 4000–4008.
[41] M. Poschmann, P. Bajpai, B.W.N. Fitzpatrick, M.H.A. Piro, "Recent developments for molten salt systems in Thermochimica, Calphad 75 (2021) 102341.
[42] J.v. Laar, The melting or solidification curves in binary systems when the solid phase is a mixture (amorphous solid solution or mixed crystals) of the two components, J. Phys. Chem. 64 (1) (1908) 257–297.
[43] P. Chartrand, A. Pelton, On the choice of geometric thermodynamic models, J. Phase Equilibria 21 (2) (2000) 141–147.
[44] P. Bajpai, M. Poschmann, M.H. Piro, Derivations of partial molar excess gibbs energy of mixing expressions for common thermodynamic models, J. Phase Equilibria Diffusion 42 (2021) 333–347.
[45] F.-Z. Roki, M.-N. Ohnet, S. Fillet, C. Chatillon, I. Nuta, Critical assessment of thermodynamic properties of CsI solid, liquid and gas phases, J. Chem. Thermodyn. 70 (2014) 46–72.
[46] M. Piro, S. Simunovic, T. Besmann, B. Lewis, W. Thompson, The thermochemistry library THERMOCHIMICA, Comput. Mater. Sci. 67 (2013) 266–272.
[47] C.N.R. Rao and M. Natarajan in Crystal Structure Transformations in Binary Halides, vol. 41, ch. 1–13, pp. 1–53, The National Standard Reference Data Series, National Bureau of Standards, U.S. Dept. of Commerce, Washington, DC, 1972.